

Convolutional neural network-based analysis of pediatric chest X-ray images for pneumonia detection

Yilou Ma¹, Ricardo A. Gonzales²

¹ Santa Catalina School, Monterrey, California, United States

² Radcliffe Department of Medicine, University of Oxford, Oxford, United Kingdom

SUMMARY

Detection of pneumonia is generally done using chest X-ray images, traditionally assessed manually by radiologists. However, this method has limitations, including the potential for human error, variability in interpretation, and a shortage of skilled professionals, particularly in resource-limited settings. Prompted by these challenges and the increasing potential of machine learning in medical diagnostics, we investigated the efficacy of advanced computational models in distinguishing between normal and pneumonia-affected lung images. We hypothesized that an adapted version of the VGG16 model, a convolutional neural network (CNN), would outperform the standard VGG16 and simpler Multilayer Perceptrons (MLPs) in terms of accuracy and reliability. Utilizing a dataset from the Guangzhou Women and Children's Medical Center, we evaluated the performance of these three models on pediatric chest X-ray images. The MLP showed moderate effectiveness with 78.4% accuracy but struggled with complex image data. The standard VGG16 achieved better results with 90.9% accuracy but displayed overfitting tendencies. The adapted VGG16 model, with reduced filter sizes and dropout layers, demonstrated the highest accuracy at 95.6%, indicating superior performance and stability. These findings suggest that tailored deep learning models like the adapted VGG16 can significantly enhance pneumonia diagnosis from chest X-ray images, offering a balance of accuracy, efficiency, and generalizability. This advancement holds substantial implications for improving diagnostic processes in pediatric healthcare, particularly in settings with limited resources.

INTRODUCTION

Pneumonia is a prevalent and potentially severe respiratory infection that inflames the air sacs in one or both lungs, leading to a range of symptoms including coughing, fever, and shortness of breath (1). It holds significant importance in global health due to its high incidence, especially among vulnerable populations like children and the elderly (2). The complexity of its symptoms, which can often resemble those of a common cold or influenza, makes accurate diagnosis crucial (3). The impact of pneumonia is especially pronounced in regions with limited healthcare resources, where it contributes

considerably to morbidity and mortality (4). Understanding and addressing pneumonia is not only a medical challenge but also a public health priority, necessitating advancements in diagnostic methods to improve patient outcomes (5).

The detection of pneumonia typically involves the use of chest X-rays, which are radiographic images of the chest used to visualize the lungs and surrounding tissues (6). Chest X-rays are considered a standard diagnostic tool in identifying lung infections and inflammations. They work by passing a small amount of radiation through the body to produce images of the internal structures (7). The varying densities of different tissues and organs, including the air in the lungs, absorb this radiation differently. This effect results in a picture that can reveal abnormalities like the consolidation characteristic of pneumonia (7). However, the interpretation of these images requires specialized knowledge and experience, as subtle differences in shading can indicate the presence or absence of disease (8).

The manual assessment of chest X-rays has limitations including the potential for human error and variability in interpretation (9). This issue is particularly pronounced in areas with a shortage of expert radiologists (10). In recent years, machine learning has emerged as a promising tool to address these challenges, beginning with multilayer perceptrons (MLPs) and evolving into more sophisticated models like convolutional neural networks (CNNs) (11, 12). MLPs, simple forms of artificial neural networks, were an initial step in automated image analysis but lacked the ability to efficiently process complex image data. CNNs, however, with their capacity for feature detection and pattern recognition in images, have shown considerable potential in enhancing the accuracy and efficiency of medical image analysis, including chest X-rays (13). Among the various CNN architectures, VGG16 has gained prominence for its depth and ability to capture intricate image features, making it suitable for complex medical image analysis (13).

The objective of this study is to evaluate the efficacy of an adapted version of the VGG16 model, a specific type of CNN, in the diagnosis of pneumonia from chest X-ray images. We hypothesized that an adapted VGG16 model would demonstrate superior performance compared to both the standard VGG16 and conventional MLPs in terms of accuracy and efficiency in pneumonia detection. We modified the VGG16 model, known for its depth and ability to process complex image data, to better suit the specific requirements of pneumonia detection in chest X-rays. Our findings indicate that the adapted VGG16 model outperformed both the standard VGG16 and MLPs, achieving the highest accuracy and stability, demonstrating its potential to improve pneumonia detection and reduce diagnostic errors, particularly in under-

resourced healthcare settings.

RESULTS

To determine if our modified VGG16 model can better identify patients suffering from pneumonia (Figure 1A) than simpler, less tailored models, we evaluated the accuracy of pneumonia diagnoses of three training models: an MLP, a standard VGG16, and an adapted VGG16 (Figure 1B-D). Each model was trained over 100 epochs, utilizing a dataset of pediatric chest X-ray images categorized as 'Normal' or 'Pneumonia' (14). This dataset consisted of 5,856 chest X-ray images from the Guangzhou Women and Children's Medical Center. The performance of the models was assessed using accuracy, which measures the proportion of correct diagnoses, and the F1 score, which provides a balanced evaluation by considering both the precision (correct identification of pneumonia cases) and recall (ability to detect all actual pneumonia cases).

The MLP model, with 4,213,121 parameters, showed a final accuracy of 78.4% and an F1 score of 83.6% on the validation set. This plateau in performance suggested a limitation in

handling the complexity of the chest X-ray images. Although the MLP model's accuracy steadily improved when tested on the training dataset, its performance was inconsistent and failed to stabilize when evaluated on the validation dataset (Figure 2A).

In comparison, the standard VGG16 model, with 65,057,473 parameters, demonstrated an improved performance, reaching an accuracy of 90.9% and an F1 score of 93.7% on the validation set. Despite better results than the MLP, the standard VGG16 model began showing overfitting tendencies post the 70th epoch. Overfitting occurs when a model learns patterns specific to the training data, causing a decline in its ability to generalize to new, unseen data. This was evident from the divergence observed between the training and validation accuracy curves. While the training and validation curves of the standard VGG16 indicated a more stable convergence than the MLP, we also observed some slight fluctuations in validation accuracy, reflecting variability in performance due to model sensitivity to specific data points (Figure 2B). We further noted that these fluctuations, along with the eventual overfitting, suggest that the model became too tailored to the training data, reducing its effectiveness on new cases.

The adapted VGG16 model, which involved modifying the standard VGG16 architecture to better suit the task of pneumonia detection, displayed a higher level of efficacy than either the MLP or original VGG16 model. This adaptation included reducing the filter sizes in the convolutional layers to balance feature extraction and computational efficiency and incorporating dropout layers to prevent overfitting by randomly omitting certain neurons during training. With 4,212,321 parameters, the adapted model achieved an accuracy of 95.6% and an F1 score of 97.1% on the validation set and maintained consistent performance throughout the training process. The training and validation accuracy curves for the adapted VGG16 remained closely aligned, suggesting minimized overfitting and enhanced capability in generalizing to new data (Figure 2C).

Statistical analysis using McNemar's test revealed significant differences in the classification performance among the three models. This test compared the performance of each pair of models—MLP versus standard VGG16, standard VGG16 versus adapted VGG16, and MLP versus adapted VGG16—by evaluating the discrepancies in their misclassifications on the same dataset. The highly significant differences ($p < 0.001$) indicated by chi-squared values of 631,362.6, 955,599.2, and 489,878.99, respectively, show that each model's accuracy in diagnosing pneumonia from chest X-rays was distinct, with the adapted VGG16 model demonstrating a clear advantage over both the standard VGG16 and MLP models.

DISCUSSION

The results of this study offer valuable insights into the application of machine learning models in medical image analysis, specifically in the diagnosis of pneumonia from chest X-ray images. The MLP demonstrated an accuracy of 78.4% and F1 score of 83.6% on the validation set. This outcome indicates a moderate level of effectiveness but also highlights the model's limitations in processing the complexity inherent in medical imaging, in line with previous findings (15). The inconsistency and failure of the validation curve to

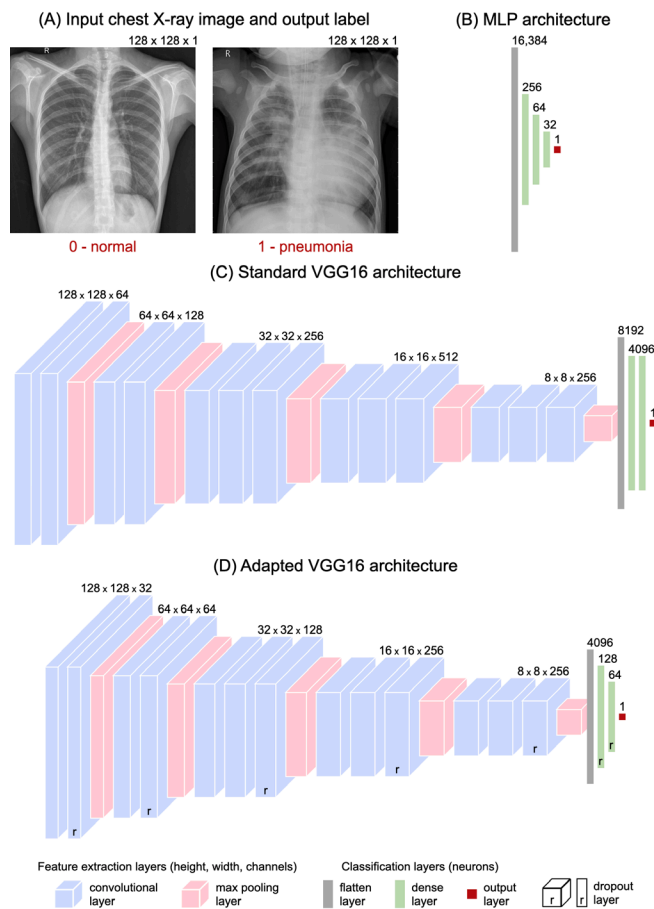


Figure 1: Classification model architectures for pneumonia detection. (A) Input chest X-ray image labeled for 'normal' (labelled as 0) or 'pneumonia' (labelled as 1), reproduced from Kermay et al. (14) under Creative Commons license CC BY 4.0, with written permission from the authors. Each image was resized to fixed width and height of 128 with one grayscale channel (128 x 128 x 1). (B) Multilayer perceptron (MLP) structure with neuron counts per layer. (C) Standard VGG16 layer configuration. (D) Adapted VGG16 model with adjusted filters, neurons and dropout layers.

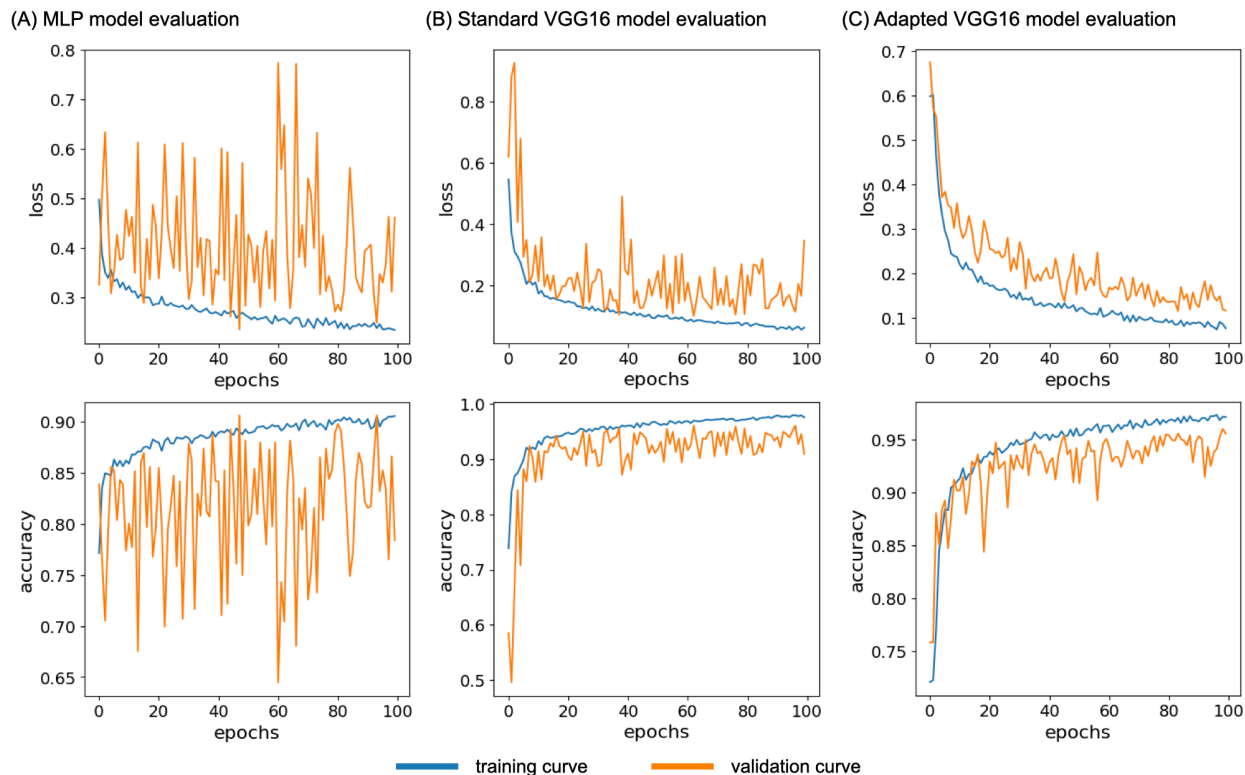


Figure 2: Performance evaluation of pneumonia detection models using a dataset of 5,856 pediatric chest X-ray images, with 80% used for training and 20% for validation. The top row shows the loss curves, and the bottom row displays the accuracy curves over 100 epochs for (A) the multilayer perceptron (MLP) model, (B) the standard VGG16 model, and (C) the adapted VGG16 model. The blue lines represent the training performance, while the orange lines indicate validation performance.

converge further underscore the challenges faced by simpler neural network architectures in tasks requiring nuanced interpretation of medical data.

In contrast, the standard VGG16 model achieved a higher accuracy of 90.9% and F1 score of 93.7% on the validation set. This marked improvement over the MLP corroborates the advantages of deep convolutional neural networks in image recognition tasks (16). However, the onset of overfitting beyond the 70th epoch, as indicated by the divergence in training and validation accuracy, suggests a limitation in the model's ability to generalize beyond the training data without adjustments. This aspect is crucial in medical applications where models must reliably interpret diverse and unseen datasets.

The adapted VGG16 model, with its reduced parameter count, not only achieved the highest accuracy (95.6%) and F1 score (97.1%) but also maintained consistent performance throughout the training. The stability of the training and validation accuracy curves reflects the effectiveness of the architectural modifications, such as reduced filter sizes and the addition of dropout layers (17). These adjustments appear to have mitigated the issue of overfitting, enhancing the model's ability to generalize to new data. This finding is particularly relevant in the field of medical diagnostics, where the robustness and accuracy of models can directly impact patient outcomes (18).

Data augmentation plays a critical role in improving the generalization of machine learning models, especially in medical image analysis where the variation in patient images can be significant (19). In this study, we employed several

augmentation techniques, applied in the three models, including rescaling, random zoom, rotation, brightness adjustment, and contrast modification. These methods were selected to mimic the variability that can occur in clinical settings due to differences in imaging equipment, patient positioning, and environmental lighting conditions. By incorporating these variations during training, the models are better equipped to handle diverse real-world data, thus enhancing their diagnostic robustness and accuracy in identifying pneumonia from chest X-ray images.

Our study's findings have broader implications for the implementation of machine learning in healthcare. The adapted VGG16 model, balancing complexity with efficiency, presents a promising approach for medical image analysis. It demonstrates the potential of tailored deep learning models to not only achieve high accuracy but also to maintain stability and generalizability in diverse clinical environments. This balance is essential for practical applications where computational resources and the need for reliable diagnoses converge (18). Furthermore, the approach used in this study extends beyond the diagnosis of pneumonia in pediatric chest X-ray images. The high-resolution and detailed imaging capabilities of MRI make it a suitable candidate for applying this deep learning approach, potentially enhancing the detection of diseases that require detailed soft tissue contrast. Such adaptations could improve the diagnosis of lung-related diseases, including various forms of cancer such as lung cancer and osteosarcoma (19). The success of the adapted VGG16 model in accurately diagnosing pneumonia underscores the importance of optimizing models for specific

use cases and suggests its potential applicability to a broader range of diagnostic challenges in pulmonary medicine. This versatility could extend to different imaging modalities and settings, affirming the transformative potential of machine learning in enhancing diagnostic processes for critical health conditions.

The study has several limitations that warrant consideration. Firstly, the dataset utilized was sourced from a single center, which may limit the generalizability of the findings across different populations and medical settings; however, we attempted to mitigate this limitation through data augmentation techniques to enhance model robustness. Additionally, the models' scope of detection was restricted to differentiating between normal and pneumonia-affected X-ray images, omitting other potential pathologies that could be present. Although the dataset size is substantial for a medical imaging study, with thousands of images, it remains small compared to other deep learning projects that often utilize millions of images, which may affect the robustness and learning capacity of the models used. Moreover, while the VGG16 model is advanced for convolutional neural network applications, the emergence of vision transformers—models that leverage self-attention mechanisms to capture long-range dependencies in image data—presents a potentially more effective alternative that was not explored in this study (21).

The application of these machine learning models in diagnosing pneumonia is an evolving field, demonstrating potential in academic settings (22). However, their transition into clinical practice has been limited by challenges such as model overfitting, generalizability across diverse patient populations, and computational demands (23). The adapted VGG16 model developed in this study is a step forward to address these issues. While the model shows promising results, indicating readiness for further clinical validation, it might require additional refinements for robustness across broader diagnostic settings. Further research should explore these optimizations to ensure the model's efficacy and reliability in real-world healthcare environments.

METHODS

Imaging dataset

The study utilized a publicly available and ethically approved dataset from the Guangzhou Women and Children's Medical Center (14). It consisted of 5,856 anterior-posterior chest X-ray images of pediatric patients aged between one and five years old. The images were classified into two categories: 1,583 images labeled as 'Normal', and 4,273 images labeled as 'Pneumonia'.

Data pre-processing

To enhance the model's processing speed while retaining essential details, each image was resized to 256x256 pixels. A binary system was employed for classification, where '0' would represent a healthy case and '1' would indicate pneumonia (**Figure 1A**). The dataset was split, with 80% used for training the model and the remaining 20% for testing its accuracy.

MLP architecture

The MLP model in our study was a type of feedforward artificial neural network known for its simplicity and

effectiveness in classification tasks (**Figure 1B**) (11). It was structured to include a flatten layer that converts 2D image data into a 1D array, suitable for input into the subsequent layers. Following this, the model comprised three fully connected dense layers containing 256, 64, and 32 neurons, respectively. Each neuron in these layers was connected to every neuron in the subsequent layer, i.e., fully connected. The 'Rectified Linear Unit' (ReLU) activation function was utilized in these layers to introduce non-linearity, enabling the model to learn more complex patterns. The architecture was completed with an output layer, which was a dense layer equipped with one single neuron that employed a 'sigmoid' activation function. This design was particularly suited for binary classification, as it produces a value between 0 and 1, effectively distinguishing between the two classes.

Standard VGG16 architecture

The standard VGG16 model was a deep convolutional neural network known for its depth and use in complex image classification tasks (**Figure 1C**) (24). Its architecture was characterized by multiple sets of convolutional 2D layers, each comprising an increasing number of filters ranging from 64 to 512. These layers were instrumental in extracting features from the input images by applying various filters that capture different aspects of the image. Following each set of convolutional layers, max pooling 2D layers were employed to reduce the spatial dimensions of the input volume, thus focusing on the most significant elements in each feature map. The architecture also included a flatten layer that transforms the 2D feature maps into a 1D vector, preparing the data for the subsequent dense layers. There were two dense layers within the model, each containing 4096 neurons, a design that enabled the network to learn complex patterns from the extensive feature maps generated by the preceding layers. The model culminated in an output layer that, akin to the MLP model, utilized a sigmoid activation function to facilitate binary classification.

Adapted VGG16 architecture

The adapted VGG16 model, a variation of the standard VGG16, was tailored to optimize performance for the specific task of analyzing chest X-ray images (**Figure 1D**). This model distinguished itself by adjusting the number of filters in its convolutional 2D layers to 32, 64, 128, and 256, a modification aimed at achieving a balance between feature extraction capability and computational efficiency. In addition, dropout layers were incorporated after selected convolutional 2D layers and dense layers, where a 30% of neurons were randomly omitted during training. This approach effectively reduced overfitting by preventing the model from becoming overly dependent on any single feature (25). Furthermore, the adapted VGG16 model simplified its dense layers by reducing the number of neurons to 128 and 64, contrasting with the standard VGG16. This adjustment helped to prevent overfitting and reduces computational load.

Data augmentation

For all three models, data augmentation techniques were applied to the input images to improve the model's generalization capabilities. By implementing these data augmentation methods, the models were trained on a more diverse set of data, helping to improve their robustness and

ability to generalize to new, unseen data (20). The techniques utilized include rescaling, random zoom, random rotation, random brightness, and random contrast adjustments. Rescaling normalized the pixel values to a range between 0 and 1 to ensure consistency in image representation. Random zoom applied varying degrees of zoom to simulate different image distances. Random rotation involved rotating the images by arbitrary angles to mimic changes in patient positioning. Random brightness and contrast adjustments modified the brightness and contrast levels to reflect different imaging conditions.

Model hyperparameters and optimization

All models were compiled using the Adam optimizer with a learning rate of 0.0001 and a binary cross-entropy loss function (26). The training process involved 100 epochs with a batch size of 32. The training and validation datasets were fed into the models for the fitting process. The intention behind these specific architectures and hyperparameter settings was to optimize each model for the best possible performance in accurately classifying the chest X-ray images. All preprocessing, development and evaluation were done using Python 3.10.12 with Tensorflow 2.15.0 (27). The code for data preprocessing, training the model, and evaluation is accessible on GitHub in the following repository: <https://github.com/nancyma07z/pneumonia-detection-project>.

Performance evaluation

The effectiveness of the baseline MLP, standard VGG16, and adapted VGG16 models is assessed based on their accuracy, F1 score, and the analysis of their training and validation curves. Overfitting is particularly monitored through discrepancies between training and validation performance. To assess the statistical significance of performance differences between the baseline MLP, standard VGG16, and adapted VGG16 models, McNemar's test was applied. This test, appropriate for paired nominal data, used a 2x2 contingency table for each pair of classifiers to analyze discrepancies in predictions against the ground truth and to highlight significant differences in their performance.

ACKNOWLEDGMENTS

We would like to acknowledge the mentorship and technical support provided by Veritas AI, which facilitated the development and refinement of this work.

Received: January 31, 2024

Accepted: June 23, 2024

Published: October 8, 2024

REFERENCES

1. Wang, Haidong, et al. "Global, Regional, and National Life Expectancy, All-Cause Mortality, and Cause-Specific Mortality for 249 Causes of Death, 1980–2015: A Systematic Analysis for the Global Burden of Disease Study 2015." *The Lancet*, vol. 388, no. 10053, Oct. 2016, pp. 1459–1544, [https://doi.org/10.1016/s0140-6736\(16\)31012-1](https://doi.org/10.1016/s0140-6736(16)31012-1).
2. Madhi, Shabir A., et al. "The Burden of Childhood Pneumonia in the Developed World." *Pediatric Infectious Disease Journal*, vol. 32, no. 3, Mar. 2013, pp. e119–e127, <https://doi.org/10.1097/inf.0b013e3182784b26>.
3. Malani, Preeti N. "Mandell, Douglas, and Bennett's Principles and Practice of Infectious Diseases." *JAMA*, vol. 304, no. 18, 10 Nov. 2010, <https://doi.org/10.1001/jama.2010.1643>.
4. Aston, Stephen J. "Pneumonia in the Developing World: Characteristic Features and Approach to Management." *Respirology*, vol. 22, no. 7, 6 July 2017, pp. 1276–1287, <https://doi.org/10.1111/resp.13112>.
5. Wunderink, Richard G, and Grant Waterer. "Advances in the Causes and Management of Community Acquired Pneumonia in Adults." *BMJ*, vol. 358, 10 July 2017, p. j2471, <https://doi.org/10.1136/bmj.j2471>.
6. Watkins, Richard R., and Tracy L. Lemonovich. "Diagnosis and Management of Community-Acquired Pneumonia in Adults." *American Family Physician*, vol. 83, no. 11, 1 June 2011, pp. 1299–1306.
7. Curry, Thomas S, et al. *Christensen's Physics of Diagnostic Radiology*. Philadelphia, Lippincott Williams & Wilkins, 1990.
8. Çalli, Erdi, et al. "Deep Learning for Chest X-Ray Analysis: A Survey." *Medical Image Analysis*, vol. 72, Aug. 2021, p. 102125, <https://doi.org/10.1016/j.media.2021.102125>.
9. Itri, Jason N., et al. "Fundamentals of Diagnostic Error in Imaging." *RadioGraphics*, vol. 38, no. 6, Oct. 2018, pp. 1845–1865, <https://doi.org/10.1148/rq.2018180021>.
10. Frija, Guy, et al. "How to Improve Access to Medical Imaging in Low- and Middle-Income Countries?" *EClinicalMedicine*, vol. 38, 1 Aug. 2021, p. 101034 <https://doi.org/10.1016/j.eclinm.2021.101034>.
11. Lakhani, Paras, et al. "Machine Learning in Radiology: Applications beyond Image Interpretation." *Journal of the American College of Radiology*, vol. 15, no. 2, Feb. 2018, pp. 350–359, <https://doi.org/10.1016/j.jacr.2017.09.044>.
12. Aggarwal, Charu C. *Neural Networks and Deep Learning: A Textbook*. Cham, Springer International Publishing, 2018.
13. Shin, Hoo-Chang, et al. "Deep Convolutional Neural Networks for Computer-Aided Detection: CNN Architectures, Dataset Characteristics and Transfer Learning." *IEEE Transactions on Medical Imaging*, vol. 35, no. 5, May 2016, pp. 1285–1298, <https://doi.org/10.1109/tmi.2016.2528162>.
14. Kermany, Daniel, et al. "Labeled Optical Coherence Tomography (OCT) and Chest X-Ray Images for Classification." *Mendeley Data*, vol. 2, June 2018, <https://doi.org/10.17632/rscbjbr9sj.2>.
15. Dutta, Suvajit, et al. "A Comparative Study of Deep Learning Models for Medical Image Classification." *IOP Conference Series: Materials Science and Engineering*, vol. 263, Nov. 2017, p. 042097, <https://doi.org/10.1088/1757-899x/263/4/042097>.
16. Abiyev, Rahib H., and Mohammad Khaleel Sallam Ma'aitah. "Deep Convolutional Neural Networks for Chest Diseases Detection." *Journal of Healthcare Engineering*, vol. 2018, 1 Aug. 2018, pp. 1–11, <https://doi.org/10.1155/2018/4168538>.
17. Anwar, Syed Muhammad, et al. "Medical Image Analysis Using Convolutional Neural Networks: A Review." *Journal of Medical Systems*, vol. 42, no. 11, Oct. 2018, <https://doi.org/10.1007/s10916-018-1088-1>.
18. Ben-Israel, David, et al. "The Impact of Machine Learning on Patient Care: A Systematic Review." *Artificial*

- Intelligence in Medicine*, vol. 103, Mar. 2020, p. 101785, <https://doi.org/10.1016/j.artmed.2019.101785>.
19. Luo, Zhendong, et al. "Radiomics Analysis of Multiparametric MRI for Prediction of Synchronous Lung Metastases in Osteosarcoma." *Frontiers in Oncology*, vol. 12, Feb. 2022, <https://doi.org/10.3389/fonc.2022.802234>.
 20. Shorten, Connor, and Taghi M. Khoshgoftaar. "A Survey on Image Data Augmentation for Deep Learning." *Journal of Big Data*, vol. 6, no. 1, 6 July 2019, <https://doi.org/10.1186/s40537-019-0197-0>.
 21. Li, Jun, et al. "Transforming Medical Imaging with Transformers? A Comparative Review of Key Properties, Current Progresses, and Future Perspectives." *Medical Image Analysis*, vol. 85, Apr. 2023, p. 102762, <https://doi.org/10.1016/j.media.2023.102762>.
 22. Sharma, Shagun, and Kalpna Guleria. "A Deep Learning Based Model for the Detection of Pneumonia from Chest X-Ray Images Using VGG-16 and Neural Networks." *Procedia Computer Science*, vol. 218, 2023, pp. 357–366, <https://doi.org/10.1016/j.procs.2023.01.018>.
 23. Chibugo, Francisca, et al. "The role of artificial intelligence in healthcare: a systematic review of applications and challenges." *International Medical Science Research Journal*, vol. 4, no. 4, Apr. 2024, pp. 500–508, <https://doi.org/10.51594/imsrj.v4i4.1052>.
 24. Simonyan, K., and A. Zisserman. "Very Deep Convolutional Networks for Large-Scale Image Recognition." 3rd International Conference on Learning Representations (ICLR 2015), 2015.
 25. Srivastava, Nitish, et al. "Dropout: a simple way to prevent neural networks from overfitting." *The Journal of Machine Learning Research*, vol. 15, no. 1, Jan 2014.
 26. Kingma, Diederik P., and Ba, Jimmy. "Adam: A method for stochastic optimization." 3rd International Conference on Learning Representations (ICLR 2015), 2015, <https://doi.org/10.48550/arXiv.1412.6980>.
 27. Abadi, Martin, et al. "TensorFlow: A System for Large-Scale Machine Learning." *12th USENIX symposium on operating systems design and implementation (OSDI 16)*, 2016.

Copyright: © 2024 Ma and Gonzales. All JEI articles are distributed under the attribution non-commercial, no derivative license (<http://creativecommons.org/licenses/by-nc-nd/4.0/>). This means that anyone is free to share, copy and distribute an unaltered article for non-commercial purposes provided the original author and source is credited.